The Journal of Experimental Biology 209, 2085-2102
Published by The Company of Biologists 2006
doi:10.1242/jeb.02266

In vivo cranial suture function and suture morphology in the extant fish *Polypterus*: implications for inferring skull function in living and fossil fish

Molly J. Markey[1,*], Russell P. Main[2] and Charles R. Marshall[1,2]

[1]*Department of Earth and Planetary Sciences and* [2]*Department of Organismic and Evolutionary Biology, Harvard University, USA*

*Author for correspondence (e-mail: markey@fas.harvard.edu)

Accepted 11 April 2006

Summary

This study describes the mechanical role that cranial sutures play in fish during feeding. The long-term goal of our work is to establish relationships between suture form and function, so that functional inferences can be made from suture morphology in fossil taxa. To this end, strain gauges were surgically implanted across selected sutures in the skull roof of four individuals of *Polypterus endlicherii*. After surgery, bone and suture strains during feeding were recorded along with high-speed video of the feeding events. Each trial was designated as a suction feeding or biting on prey trial, and neurocranial elevation, hyoid position and gape were quantified to aid in interpreting the strain data. The strains due to suction feeding are different from those observed during biting. Suction feeding results in a fairly stereotyped strain pattern, with the interfrontal and frontoparietal sutures experiencing tension, while the interparietal suture is compressed. Biting causes much more variable strain patterns. However, both suction and biting result in compression in the back of the skull, and tension between the frontals. Peak strains, and the time at which they occur in the feeding cycle, were compared between suction and biting. In general, peak suture strains are higher during suction than during biting, but not all of these differences are significant. Peak suture and bone strains occur at or near maximum gape during both suction and biting, suggesting that these strains are caused by muscle contraction involved in mouth opening and closing. Micro-computed tomography (microCT) scans of the experimental specimens indicate that the interfrontal and frontoparietal sutures, typically loaded in tension, are less interdigitated in cross section than the interparietal suture, which experiences compression. This is consistent with published correlations of suture form and function in mammals, where interdigitated sutures indicate compression and lack of interdigitation is associated with tension.

Supplementary material available online at
http://jeb.biologists.org/cgi/content/full/209/11/2085/DC1

Key words: cranial, suture, skull, *Polypterus endlicherii*, bone strain, suction feeding.

Introduction

'*Polypterids are well able to catch fast swimming fish by an elegant mode of suction feeding…however, used to easily available dead and benthic prey in aquaria, they will seldom show their full repertoire of prey capture*.' (Bartsch, 1997)

Several paleontologists have hypothesized that the morphology of cranial sutures (the fibrous joints between bones of the skull) of fossil fish and amphibians may capture information about skull function during feeding (Thomson and Bossy, 1970; Beaumont, 1977; Thomson, 1993; Thomson, 1995; Kathe, 1999; Clack, 2002; Clack, 2003). In particular, many studies have focused on using the distribution of suture types in the skulls of extinct fish and amphibians to reconstruct patterns of force transmission (Thomson, 1995; Kathe, 1999; Clack, 2003), with the aim of linking these patterns to specific feeding modes. Using this approach, it may be possible to infer feeding methods employed by fossil taxa whose skull morphology is far removed from that of living species; for example, the extinct amphibian *Diplocaulus*, which exhibits an unusual 'boomerang'-shaped skull (Carroll, 1988).

In addition, cranial suture shape may provide new insights into changes in skull function during evolutionary transitions. For example, Clack has suggested (Clack, 2002) that the heavily interdigitated sutures of the tristicopteryid fish *Panderichthys* may reflect an increasingly terrestrial lifestyle. The shift from relatively straight to interdigitated sutures during the fish–amphibian transition – that is, between *Eusthenopteron* and *Acanthostega* – has also been attributed to changes in feeding type or, alternatively, to differences in the preferred environment of these taxa (Clack, 2002; Clack, 2003).

However, the paleontological studies discussed here rely on

correlations of suture form and function observed in living mammals to make inferences about fossil fish and amphibians (e.g. Kathe, 1999), because no experiments have been conducted on extant fish or amphibians to determine if there is a link between suture form and function during feeding in these groups.

In vivo strain measurements across sutures in several mammalian taxa, including macaques (Behrents et al., 1978; Bourbon, 1982), miniature pigs (Herring and Mucci, 1991; Rafferty and Herring, 1999; Herring and Teng, 2000; Sun et al., 2004), goats (Jaslow and Biewener, 1995) and hyraxes (Lieberman et al., 2004), and studies of reptiles including monitor lizards (Smith and Hylander, 1985) and alligators (Metzger and Ross, 2004), have established that the shape of cranial sutures is in part determined by the forces experienced by the skull, particularly by the low-magnitude but repetitive forces generated by muscle contraction during mastication (Behrents et al., 1978; Bourbon, 1982; Herring and Mucci, 1991; Rafferty and Herring, 1999; Herring and Teng, 2000; Thomason et al., 2001). The mechanism by which forces on the skull influence suture shape is unclear, because suture growth rates have not been convincingly associated with strain polarity (i.e. tension *vs* compression) or strain magnitude (Sun et al., 2004; Herring and Ochareon, 2005). However, a correlation between sutural interdigitation (viewed in cross-section) and compressive loads has consistently been reported in miniature pigs. Similarly, tension across a suture has been convincingly associated with sutures that appear straight in cross-section (see Herring and Ochareon, 2005).

This study has three major aims: (1) to measure deformation within and between skull bones during feeding in the fish *Polypterus endlicherii* [(Heckel, 1847), cited in www.fishbase.org] using strain gauges; (2) to provide hypotheses for the mechanics producing the measured deformations, based on skull anatomy and cranial muscle activity patterns during feeding in *Polypterus* from available data in the literature; and (3) to present a preliminary description of the cranial sutures in *Polypterus* using micro-computed tomography (microCT) scans of the experimental specimens and, to the extent possible, establish a link between suture anatomy and suture function during feeding. The long-term goal of this work is to establish relationships between suture form and function in extant fish, so that functional inferences can be made from suture morphology in fossil taxa.

Fish obtain their food using a wide variety of methods, including suction feeding, ram feeding, filter feeding and biting, which are not necessarily mutually exclusive (Gerking, 1994). Due to the widespread utilization of suction feeding in fishes, the majority of research on prey capture in fishes has focused on this method of obtaining food (Grubich, 2001; Gerking, 1994) (for a review, see Ferry-Graham and Lauder, 2001). Therefore our knowledge of all aspects of suction feeding – e.g. fluid mechanics (Muller and Osse, 1984; Ferry-Graham and Lauder, 2001), kinematics (Liem, 1978; Lauder, 1980; Westneat, 1990; Grubich, 2001) and muscle activities (Lauder, 1980; Lauder and Gillis, 1997) – surpasses what we know about alternative prey capture strategies. However, recent work has expanded our knowledge of additional fish feeding techniques, such as prey acquisition by oral jaw biting (Alfaro et al., 2001). In this study, both suction feeding and oral jaw biting are analyzed.

Based on the anatomy of the skull in *Polypterus* (Allis, 1922), and descriptions of suction prey capture and biting prey processing exhibited by this species (Lauder, 1980), we hypothesize that strains due to biting will exceed strains measured during suction feeding, because the major mouth closing muscles (adductor mandibulae) are much larger than the muscles employed during suction. In addition, we expect that maximum strain during suction will occur at or near maximum gape, while biting will result in maximum bone and suture deformation when the prey item is held between the jaws. We also hypothesize that interdigitated sutures in *Polypterus* will be associated with compression, while abutting sutures (i.e. flat contacts between skull bones) will be loaded in tension. Previous descriptions of the skull of *Polypterus* (Allis, 1922; Lauder, 1980) do not focus on suture morphology in sufficient detail for us to predict the morphology of the sutures examined here; however, we hypothesize that midline sutures will be more similar in shape to each other than they are to coronally positioned sutures, as is the case in mammals (Ogle et al., 2004).

Materials and methods

Four individuals of the ray-finned fish species *Polypterus endlicherii* Heckel 1847 (Chondrostei: Polypteriformes) were selected for this study (mean body length=27.1±3.0 cm). *Polypterus* was chosen due to its basal position within the Actinopterygii (Venkatesh et al., 1999; Noack et al., 1996), and its well-ossified, robust skull. In addition, the skull roof bones in these individuals are large enough that strain gauges could be implanted across coronal as well as sagittal sutures.

It is generally agreed that the largest midline bones in the skull roof of *Polypterus* are the frontals [which are homologous to the parietals of tetrapods (see Janvier, 1996; Jarvik, 1947; Allis, 1922)]. However, there is some debate about the developmental origin of the ‘parietals’ in *Polypterus*; Jarvik refers to these bones as the parietosupratemporointertemporals (Jarvik, 1947), while Allis names them parietodermopterotics (Allis, 1922). Throughout this paper, these bones are simply referred to as ‘frontals’ and ‘parietals’, terms that do not fully reflect their developmental origin but indicate their position in the skull.

In this study, skull and cranial suture deformation are measured during prey capture *via* suction. The use of suction was assessed visually from high-speed videos, and from kinematic measurements during feeding episodes. In addition, strains in and between skull bones were analyzed during oral jaw biting on a prey item that occurred after the prey had been partially sucked into the buccal cavity, and also during mastication (in which the food was fully inside the mouth).

These different feeding modes are described in more detail below (see Results).

Strain gauge preparation

One rosette strain gauge (FRA-1-11; Sokki Kenkyujo Co., Ltd., Tokyo, Japan) and three single-element (two FLA-05-11 and one FLG-02-11) strain gauges were prepared by soldering 35 cm lengths of insulated wire (36-gauge, etched Teflon^{TM} insulation; Micromeasurements, Raleigh, NC, USA) to each tab. These long lead wires were necessary to allow the fish to swim freely in its 57 liter aquarium after strain gauge implantation; however, the lead wires for all four gauges were twisted together to prevent tangling. Two layers of waterproof insulation (M-Coat A and D; Micromeasurements) were applied to each gauge. The ends of the leads were soldered to a 12-pin connector (AMP, Tyco Electronics, Harrisburg, PA, USA).

Surgery

Only two previous studies have measured bone strain in fishes (Lauder and Lanyon, 1980; Lauder, 1982), and neither of these studies includes measuring strain in the skull roof or across sutures. Therefore, we adapted the strain gauge implantation procedure described previously (Herring and Mucci, 1991), following the general surgical techniques employed by Lauder and Lanyon (Lauder and Lanyon, 1980; Lauder, 1982).

Prior to surgery, the fish were anesthetized by immersion in a buffered 0.3 g l^{-1} solution of MS-222 (tricaine methane sulfonate; Argent Chemical Laboratories, Redmond, WA, USA). Typically, immersion for 20–25 min was sufficient for full anesthesia. The fish were then moved to a surgical tray containing a 0.1 g l^{-1} MS-222 solution. Because the dorsal surface of the skull must remain dry during strain gauge implantation, the MS-222 solution was shallow enough to expose the top of the head while keeping the gills submerged. If the fish began to wake up during surgery, it was returned to the 0.3 g l^{-1} MS-222 solution until it lost its roll stability and muscle tension. Under full anesthesia, the fish retained the ability to move their operculi; however, water was pumped across the gills using a syringe every few minutes during surgery to ensure the fish were receiving enough oxygen. Opercular movement and gill color were monitored throughout the surgery.

Single-element strain gauges were bonded across the interfrontal (IF), frontoparietal (FP) and interparietal (IP)

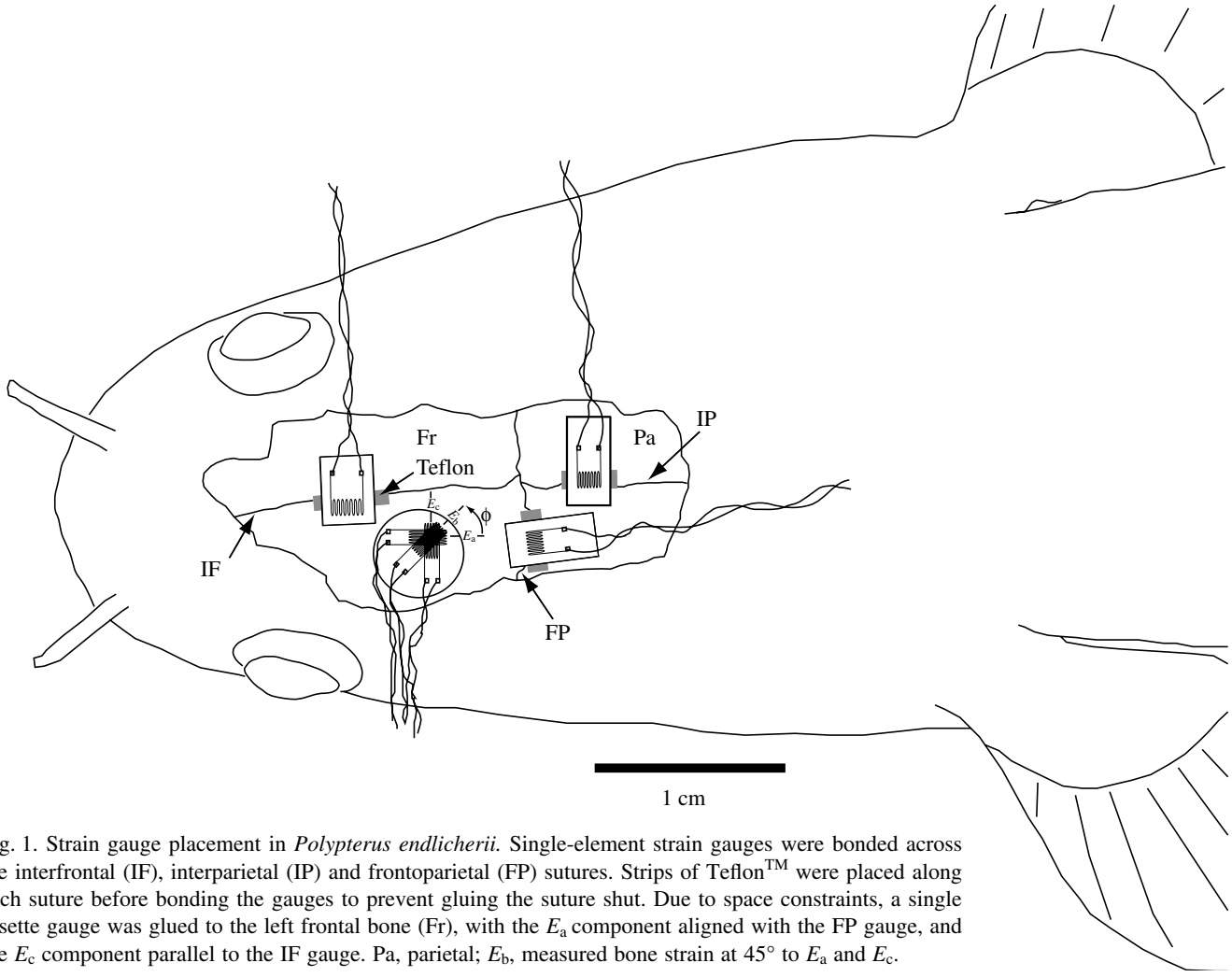

Fig. 1. Strain gauge placement in *Polypterus endlicherii.* Single-element strain gauges were bonded across the interfrontal (IF), interparietal (IP) and frontoparietal (FP) sutures. Strips of Teflon^{TM} were placed along each suture before bonding the gauges to prevent gluing the suture shut. Due to space constraints, a single rosette gauge was glued to the left frontal bone (Fr), with the E_a component aligned with the FP gauge, and the E_c component parallel to the IF gauge. Pa, parietal; E_b, measured bone strain at 45° to E_a and E_c.

sutures as shown in Fig. 1. On the selected portion of each suture, the scales and skin were scraped off using a periosteal elevator to expose the skull roof bones. No muscles insert on the dorsal surface of the skull roof at the regions of interest; therefore, gauge implantation did not disturb any cranial muscles. As a consequence of the tight connection between the skin and the dorsal surface of the skull roof in *Polypterus*, the skin cannot be replaced after being scraped off. Following exposure of the sutures of interest, the bones were dried with sterile cotton swabs and degreased with methyl ethyl ketone (Sigma Chemical Co., St Louis, MO, USA). After the bone surfaces were prepared, a thin strip of Teflon™ was placed lengthwise over each suture, to isolate the gauge from the underlying sutural tissue and prevent gluing the suture shut, following published procedures (Herring and Mucci, 1991). Single element strain gauges were bonded with a self-catalyzing cyanoacrylate glue (Duro, Henkel Loctite Corp., Rocky Hill, CT, USA) across the IF (gauge type: FLG-05-11), FP and IP (gauge type: FLA-05-11) sutures, on top of and perpendicular to the Teflon™ strips (see Fig. 1). The rosette gauge was bonded to the surface of the left frontal bone, with component E_a aligned with the FP gauge (therefore, component E_c is parallel to the IF gauge; see Fig. 1). Measurements made by the rosette gauge allow the magnitude and direction of the maximum tensile ($E1$) and minimum compressive ($E2$) principal strains experienced by the frontal bone to be assessed.

After surgery, the fish were moved to a recovery tank and monitored until they began swimming normally. Usually, normal swimming was achieved within 20 min after surgery.

Data collection

Once the fish recovered from surgery, they were moved to their original aquaria for data collection. The fish were typically unwilling to feed for 24 h after surgery. However, after that time, the fish accepted live earthworms. The lead wires for each strain gauge were connected to a shielded cable (NMUF6/30-4046SJ; Cooner Wire, Chatsworth, CA, USA), which was in turn connected to a bridge amplifier (Vishay 2120; Micromeasurements). During feeding episodes, strain data were sampled at 5000 Hz through a 12-bit A/D converter (Digidata 1200B, Axon Instruments Inc., Union City, CA USA). High-speed video of the feeding events was recorded in lateral view, using a Redlake Motionscope digital camera (Redlake Motionscope PCI, San Diego, CA, USA). A record rate of 60–125 Hz, and shutter speeds of 1/60, 1/250 or 1/500, were used depending on the individual fish analyzed. Decreasing the record rate and shutter speed was necessary to collect data from individuals that would not feed under bright lights, in spite of efforts to acclimatize them to increased light levels. [*Polypterus* feed at night in the wild (Bartsch, 1997); therefore, our fishes' reluctance to feed under bright light was not unusual.] The high-speed video recordings were synchronized with the strain data using a trigger that simultaneously sent an electrical signal to the A/D board and the camera. These videos were used to describe and quantify the feeding types exhibited by the fish, and link the observed strain patterns with the fish's activity.

Although the rosette, IF and FP gauges remained bonded in all four fish throughout data collection, complete IP data were only collected from three of the four individuals.

After data collection, the fish were euthanized by an overdose of MS-222 (immersion in 1.25 g l^{-1} MS-222 solution) for morphological study.

All experimental procedures used in this study were approved by the Institutional Animal Care and Use Committee at Harvard University (protocol 23-10).

Data analysis

Using the high-speed video, each feeding event was qualitatively characterized as suction feeding, or biting on the prey item (i.e. prey capture or manipulation in which suction was not used; lateral head motion frequently accompanied these events), or processing bites (biting motions made by the fish after the prey item was completely in the mouth). The presence of suction (S) during prey capture was inferred if the prey was seen to accelerate into the mouth with the fish's body held stationary. In certain suction feeding events, the fish seemed to close its jaws more firmly on the prey item than in other events in which suction was employed; these events were described as 'suction plus biting' (SB). Feeding events in which the fish did not employ suction, but simply compressed the prey item between its jaws, were classified as biting (B). Instances of biting with the prey item completely in the mouth were termed 'processing bites' (P). A total of 148 feeding events were recorded.

Fifty-two feeding events were selected for this study on the basis of high-speed movie quality (see Table S1 in supplementary material for a summary of these events). To aid in statistical analysis, an average of six suction and six biting events were selected for each individual. Feeding events were included in this study only if the fish was fully lateral to the camera and stayed within the field of view until feeding was complete.

High-speed video of these 52 events was used to quantify feeding activity by measuring hyoid excursion, head lifting angle, and size of gape throughout each feeding sequence. To ensure that the kinematic measurements were comparable across individuals, hyoid depression (mm) was measured level with the posterior margin of the eye in all fish. In addition, the angle of head lifting was measured between the horizontal and a line defined by the base of the right nostril tube and the posterior margin of the frontoparietal gauge. As a consequence of using these landmarks, head lifting values varied from –18° to 22°, with zero head lifting (i.e. the fish's lower jaw resting on the bottom of the tank) denoted by –18°. Finally, gape amount (mm) was assessed by measuring the distance between the tips of the jaws. All measurements were made using ImageJ 1.32j (NIH, Bethesda, MD, USA). These kinematic measurements were used to interpret the strain data, and to determine whether feeding events considered to be different were in fact measurably different (e.g. S *vs* SB events).

Previous studies have established that prey capture *via* suction can be divided into four stages, the preparatory, expansive, compressive and recovery phases (Lauder and Reilly, 1994). The preparatory phase, which has only been observed in derived percomorph taxa (Lauder, 1985), involves slight activity in muscles that open (geniohyoideus) and close (adductor mandibulae) the jaw, but the mouth remains closed throughout this phase. The expansive phase is defined as the time from the initiation of mouth opening until maximum gape, while the compressive phase is from maximum gape until the mouth is completely closed. Typically, the hyoid remains lowered even after the mouth has finished closing; therefore, the final phase of suction feeding – the recovery phase – is defined as the time from mouth closing to the return of the hyoid, suspensorium, and operculi to their initial positions (Lauder and Gillis, 1997).

The preparatory phase has not been observed in *Polypterus* (Lauder, 1980), and was not observed in this study; therefore, the preparatory phase is not included in this analysis. In addition, the recovery phase is not formally included in this study because the hyoid rarely adducted completely between closely timed events, and the position of the suspensorium and operculi could not be accurately measured because dorsal views were not recorded. However, the expansive and compressive phases were easily identified in our high-speed videos, and are used to interpret the suture and bone strains obtained during both suction feeding and biting.

Custom Matlab programs (The Mathworks, Inc., Natick, MA, USA) were used to convert the raw strain data from volts (V) to microstrains ($\mu\epsilon$) based on a 1000 $\mu\epsilon$ shunt-calibration of the Vishay bridge amplifiers. The data were also filtered using a fourth order, zero-lag Butterworth filter with a cut-off frequency of 50 Hz to remove any noise in the signal. For the single-element gauges, the direct output of these programs was used for analysis. For the rosette gauge, the program calculated the maximum (tensile) and minimum (compressive) principal strains and their orientations relative to the E_a component.

In this study, only peak strain magnitudes were analyzed because it is expected that these will have the greatest impact on suture function (see Herring and Teng, 2000). We do, however, report the frequency of smaller strain maxima during both suction and biting (see 'Results').

Statistical analyses

Statistical analyses of the strain data were used to separate differences in the mean peak suture and bone strains due to suction or biting from differences due to individual variation. The following questions were addressed: Within a given feeding mode (suction or biting), does a specific suture exhibit significantly different peak strains among the four individuals analyzed? In addition, within suction or biting, do the IP, FP and IF sutures and the frontal bone experience equivalent deformation? Finally, are there differences between feeding modes in the suture and bone strain magnitudes that are common to all four fish?

If the forces exerted on the skull by suction and biting are primarily due to muscle contraction, then peak strains should coincide with maximum gape, at the transition between the expansive and compressive phases. However, if the act of biting on a prey item involves higher forces than simply closing the mouth, peak strains in biting events should occur when the prey item is compressed between the jaws. Therefore, statistical tests were used to examine the times at which peak strains were achieved during the feeding cycle in suction and biting, and determine the effect of individual variation.

To answer the question of whether there are significant differences among individuals in peak suture and bone strain magnitude and timing within a given feeding mode, the suction and biting datasets were each subjected to a MANOVA (GLM, SPSS 12.0, Chicago, IL, USA), with individual as the independent variable, and peak IF, FP, *E*1 and *E*2 strain magnitudes or timing of these maxima as dependent variables. Due to the problem of missing data for the IP suture, a separate ANOVA was conducted for the IP suture, using fish number as the independent variable.

Paired *t*-tests were used to compare the mean strain magnitude and timing of the IP, IF and FP sutures, and *E*1 and *E*2 within each feeding mode, to determine if all parts of the skull deform similarly, at the same time.

To address the question of differences in strain magnitude and timing between suction and biting, the entire dataset (suction and biting events combined) was subjected to a MANOVA (GLM, SPSS 12.0), with individual and feeding type as independent variables, and IF, FP, *E*1 and *E*2 peak strain magnitudes or timing of these strain maxima as dependent variables. A separate one-way ANOVA (SPSS 12.0) was calculated for the IP suture strain magnitudes or timing, considering fish number as the independent variable.

Finally, the question of correlation between the timing of the fish's activity during feeding and the strain peaks observed was addressed by calculating partial correlation matrices for suction and for biting, including time of maximum head lifting, gape, hyoid lowering, maximum IP, FP and IF suture strains, and *E*1 and *E*2 bone strains.

Computed tomography scanning of experimental specimens

The skulls of all four *Polypterus* specimens were subjected to high-resolution micro-computed tomography (microCT) scanning at the Orthopedic Biomechanics Laboratory, Beth Israel Deaconess Medical Center, Boston, MA, USA. A desktop cone-beam microCT scanner (μCT40, SCANCO USA, Inc., Southeastern, PA, USA) was used to scan the specimens. The CT dataset for each specimen contains approximately 1000 slices, each 36 μm thick. These scans were used to qualitatively assess the shapes of the IF, FP and IP sutures in cross section. A quantitative treatment of the morphology of these sutures will be the focus of future study.

Results

When the fish were simply breathing or resting, the strain gauges recorded zero strain across each suture and within the

left frontal bone. Therefore, the baseline strain for all gauges was zero. Typical strain traces, and the kinematics of suction and biting events, are described below. Positive strains are tensile, while compression is expressed as negative strain.

Suction feeding

Kinematics

The kinematics of suction feeding events in *Polypterus* have been described and quantified (Lauder, 1980). In that study, measurements of hyoid depression, neurocranial elevation, gape size and opercular adduction/abduction were synchronized with high-speed video and cranial muscle activity during feeding. The amount and timing of hyoid depression, neurocranial elevation and gape during suction feeding events measured here correspond well with those presented elsewhere (Lauder, 1980).

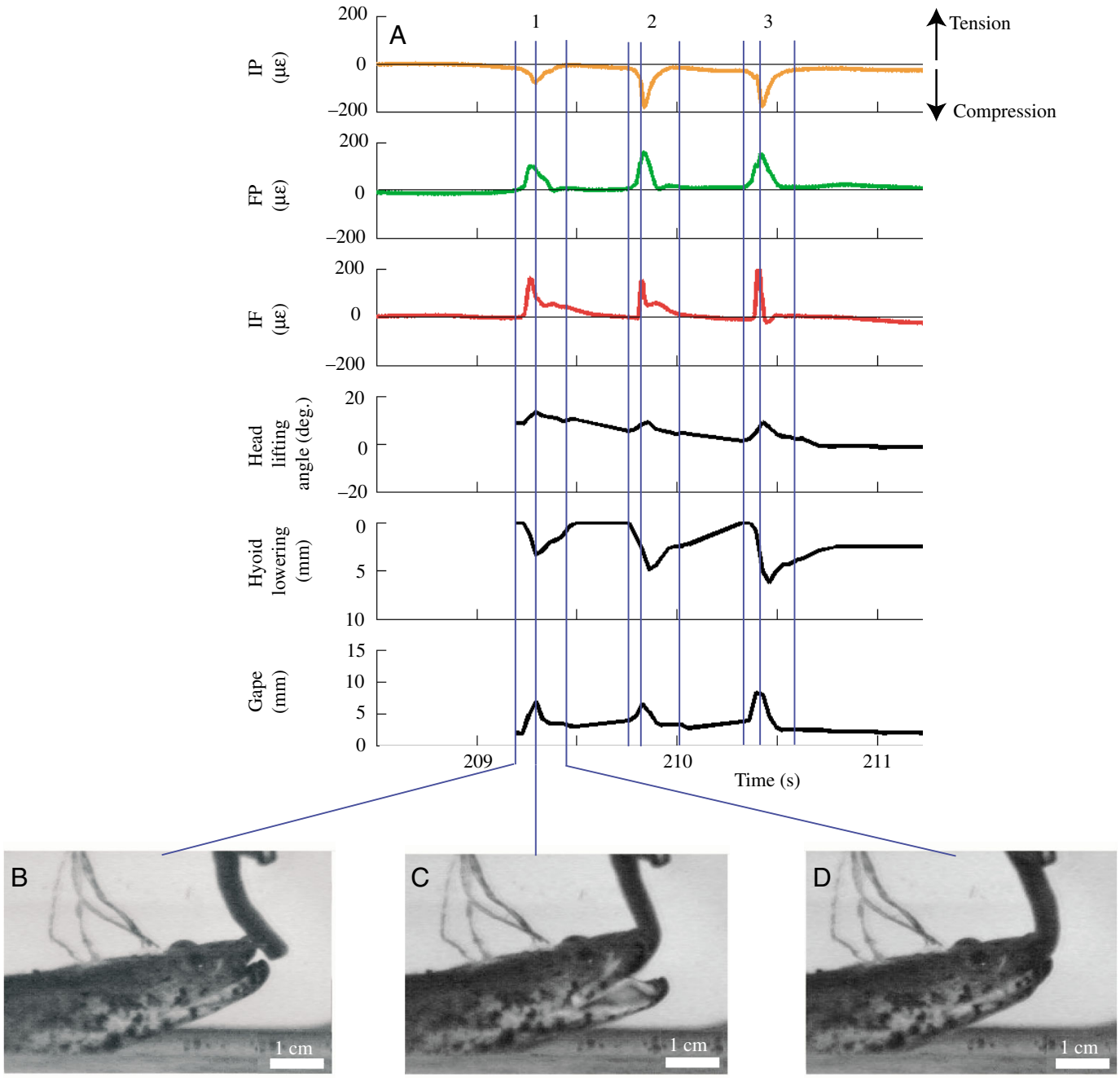

Fig. 2. (A) Kinematics and sutural strains measured during three suction feeding events (*Polypterus* 1, trial 3, events 1–3; see Table S1 in supplementary material). Still frames of (B) mouth opening, (C) maximum gape and (D) mouth closing are shown for the first suction feeding event. The blue vertical lines indicate the timing of the gape cycle. All strain peaks appear to coincide with maximum gape, and only one peak is observed in each feeding event. The interparietal (IP) suture is loaded in compression, while the interfrontal (IF) and frontoparietal (FP) sutures are loaded in tension.

Suction feeding events (S) and suction followed by biting (SB) were characterized by a large degree of head lifting and hyoid lowering during the expansive phase (head lifting=3.9±7°; hyoid depression=4.4±1.2 mm; mean ± s.d., *N*=4) (S event: first feeding event in Fig. 2; SB event: second event in Fig. 2). Lateral head motion was generally absent. Maximum gape occurred at 40±8% through the feeding cycle, while head lifting occurred slightly later at 48±7% (mean ± s.d., *N*=4). The hyoid was not fully lowered until 74±12% (mean ± s.d., *N*=4) through the feeding cycle, and often remained lowered after the mouth had completely closed. Maximum hyoid excursion in this study occurred at 49.5±33 ms after maximum gape, about 32 ms later in the feeding cycle than observed by Lauder (Lauder, 1980). However, the large standard deviation in the timing of maximum hyoid lowering means that Lauder's measurements fall within the range of variation of our data.

Based on the maximum values of hyoid excursion and head lifting angle measured here, suction feeding events (S) and suction plus biting events (SB) were indistinguishable from one another (*t*-tests; hyoid lowering, *P*=0.061; head lifting, *P*=0.484). However, maximum gape during SB events was significantly larger than during S events (*t*-test; *P*=0.006). In addition, maximum gape, hyoid excursion and head lifting angle occurred at the same times in the feeding cycle during S and SB events (*P*=0.654, *P*=0.771 and *P*=0.868, respectively). Due to the overall similarity of S and SB events, we decided to combine them into a single category. Therefore, S and SB events are both referred to as simply 'suction feeding' for the remainder of this paper.

In addition, no difference was observed in the amount and timing of neurocranial elevation (*t*-tests; amount, *P*=0.253; timing, *P*=0.487) and gape (*t*-tests; amount, *P*=0.314; timing, *P*=0.077) between suction feeding during initial strikes and suction during prey manipulation. Although maximum hyoid depression occurred significantly later in initial strike suction events (*t*-test; *P*=0.045), the amount of hyoid depression seen in both types of suction events was identical (*t*-test; *P*=0.165). Therefore, in this study, suction feeding events include initial strikes, in which the prey item is captured, and subsequent prey manipulation events, in which suction is employed (see Fig. 2).

Strain patterns

Five distinct suture strain patterns were observed during suction feeding (Table 1). Interestingly, two of these patterns account for 75% of the suction feeding events in this study (Fig. 3). In 50% of suction events, the IP was loaded in compression, while the FP and IF experienced tension. In an additional 25% of suction feeding events, the IP and FP were compressed, while the IF was loaded in tension.

If each suture is considered independently, a clear association between strain polarity and suture emerges (Table 2). During suction, the IP suture was loaded in compression in 100% of trials, while the FP experienced tension 56% of the time. It should be noted that 31% of the non-tension results for the FP were collected in a single individual (fish no. 3). In addition, the IF suture experienced tension in 94% of suction feeding events. This association of compression with the IP suture, and tension across the IF suture, is also apparent in a typical strain trace collected during suction (Fig. 2).

Multiple strain peaks were noted in 23% of suction feeding events; these include changes in strain polarity across a single suture (i.e. a tension peak followed by a compression peak, or *vice versa*) and multiple tension or multiple compression peaks occurring on a single suture during a given event. However,

Table 1. *Summary of strain patterns observed during suction and biting in Polypterus*

Fish no.		Strain pattern				
Suction	Biting	IP	FP	IF	Suction	Biting
1, 2	1, 2	Compression	Tension	Tension	8, 50%	2, 14%
3	(1)	Compression	Compression	Tension	4, 25%	1, 7%
1, 2	(2)	Compression	Tension then compression	Tension	2, 13%	1, 7%
(3)		Compression	Compression then tension	Tension	1, 6%	
(1)		Compression	Tension	Zero strain	1, 6%	
	1	Compression then tension	Tension then compression	Tension		2, 14%
	1	Compression then tension	Compression	Tension		2, 14%
	1	Compression then tension	Tension	Tension		2, 14%
	(3)	Compression	Tension	Compression		1, 7%
	(3)	Compression	Compression	Compression		1, 7%
	(3)	Compression	Tension	Tension then compression		1, 7%
	(3)	Zero	Zero	Zero		1, 7%

Data from fish nos 1–3 are combined. Fish no. 4 is omitted because the IP gauge in that fish detached during data collection.

Parentheses indicate that this strain pattern was observed just once, in only one individual.

IP, interparietal; FP, frontoparietal; IF, interfrontal.

The number and percentage of events exhibiting each strain pattern are shown for suction and biting (right). In addition, the fish in which each strain pattern is observed during suction or biting is shown (left).

For suction, *N*=16. For biting, *N*=14.

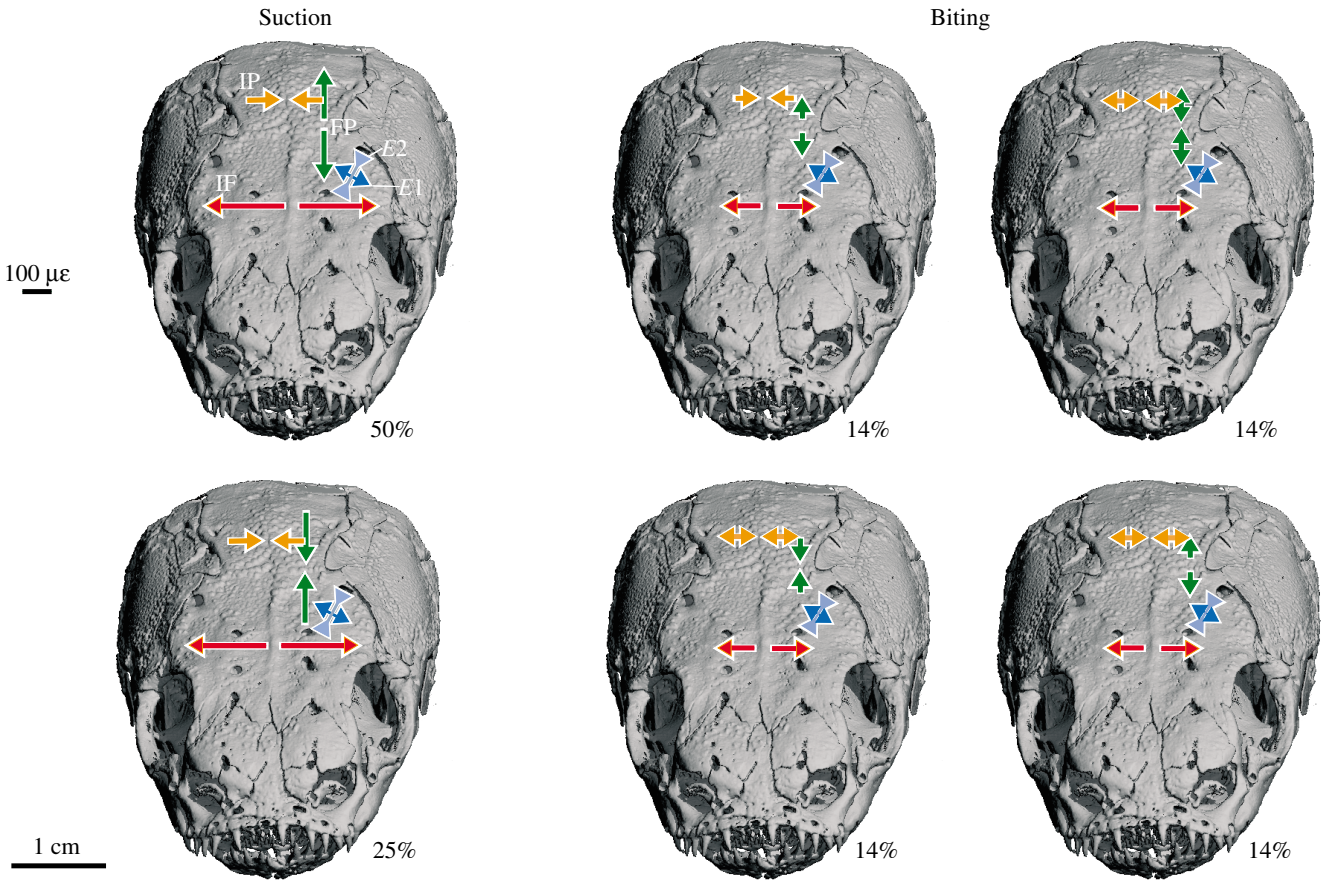

Fig. 3. Most common strain patterns during suction and biting in *Polypterus*, mapped onto a three-dimensional reconstruction of the skull made from the microCT scan of fish no. 2. Lengths of vectors are proportional to the strains they represent (see scale bar). The percentages indicate how frequently each pattern is observed during suction and biting. Double-headed arrows indicate a shift in strain polarity within a single event. In spite of the variation in strain patterns in suction and biting, the interfrontal (IF) is consistently loaded in tension, while the interparietal (IP) is compressed. The frontoparietal (FP) suture may be loaded in tension or compression, or may shift from one to the other, within a single feeding event. The maximum (*E*1) and minimum (*E*2) principal strains on the left frontal bone are also shown.

these secondary peaks were not observed to be associated with any specific activity of the fish, judging from our measurements of neurocranial elevation, gape, and hyoid excursion.

Strain magnitudes

Maximum strains due to suction feeding were significantly different among fish (MANOVA; P=0.000). However, not every suture exhibited a different peak strain in all four individuals. Instead, peak strains across the FP (ANOVA; P=0.002) and IP (ANOVA; P=0.036) sutures varied among fish, while maximum strain at the IF suture, and the maximum (tension) and minimum (compression) principal strains, did not exhibit inter-individual variation (ANOVAs; IF, P=0.329; E1, P=0.105; E2, P=0.220). However, variation in the mean strain peak magnitude across the FP and IP sutures appears to be due to one individual; specifically, fish no. 3 exhibited drastically different IP values, while fish no. 4 showed unusually high FP strains (see Fig. 4; filled symbols).

During suction, maximum IF strain (284±108 με) was greater than FP strain (161±89 με), which in turn exceeded IP strain (–100±56 με) (mean ± s.d., N=4). Although these differences in magnitude were not significant (paired t-tests; IF>FP, P=0.268; FP>|IP|, P=0.166; IF>|IP|, P=0.122), this general trend can clearly be seen in Fig. 4. Therefore, suture strain increased posterior-to-anteriorly along the skull.

Comparing suture and bone strains due to suction reveals that the maximum strain measured across the IF suture (284±108 με; mean ± s.d.; N=4) was significantly larger than the maximum strain recorded by the E_c component of the rosette (58±57 με; mean ± s.d.; N=4) (t-test; P=0.009). Although these gauges are parallel to one another, they do not lie within the same coronal plane (see Fig. 1). In addition, maximum FP strain was larger than the maximum strain experienced by the similarly aligned E_a rosette component (FP: 161±89 με; E_a: –7±28 με; mean ± s.d.; N=4); however, this difference was not significant (t-test; P=0.061). Therefore, the IF and FP sutures experienced larger tensile strains than the frontal bone during suction feeding, but not all of these differences in magnitude were significant (see Fig. 4).

Table 2. *Strain polarity observed across each suture, considered individually, during suction and biting in fish nos 1–3*

	Strain polarity (%)		
	IP	FP	IF
Suction			
Compression	100	25	
Tension		56	94
Tension then compression		13	
Compression then tension		6	
Zero strain			6
Biting			
Compression	50	29	14
Tension		43	71
Tension then compression		21	7
Compression then tension	43		
Zero strain	7	7	14

For suction, N=16. For biting, N=14.
IP, interparietal; FP, frontoparietal; IF, interfrontal.
Fish no. 4 is omitted because the IP gauge in that fish detached during data collection.

The orientation (ϕ) of maximum principal strain ($E1$) on the frontal bone changed during each suction feeding cycle; however, when the peak $E1$ value was achieved it was oriented an average of 62±2.8° to the long axis of the left frontal bone (mean ± s.d., N=4) (Figs 1, 3). The orientation (ϕ) of the maximum (tension) principal strain at its peak in each suction feeding event is provided in Table S1 in supplementary material.

Timing of strain peaks

The time at which maximum strains were achieved at the FP and IF sutures and within the left frontal bone ($E1$ and $E2$) varied significantly among fish (MANOVA: P=0.001; ANOVAs: FP, P=0.007; IF, P=0.026; $E1$, P=0.020; $E2$, P=0.040). Interestingly, a single individual is the source of all this variation in timing. If fish no. 4 is removed from the dataset, no significant difference is found in the timing of peak strain across the FP and IF sutures and within the frontal bone (MANOVA excluding fish no. 4: P>0.05 for FP and IF, $E1$ and $E2$). In addition, maximum IP strain occurred at the same point in the gape cycle in all fish (ANOVA: P=0.416).

As expected from the strain traces provided (see Fig. 2),

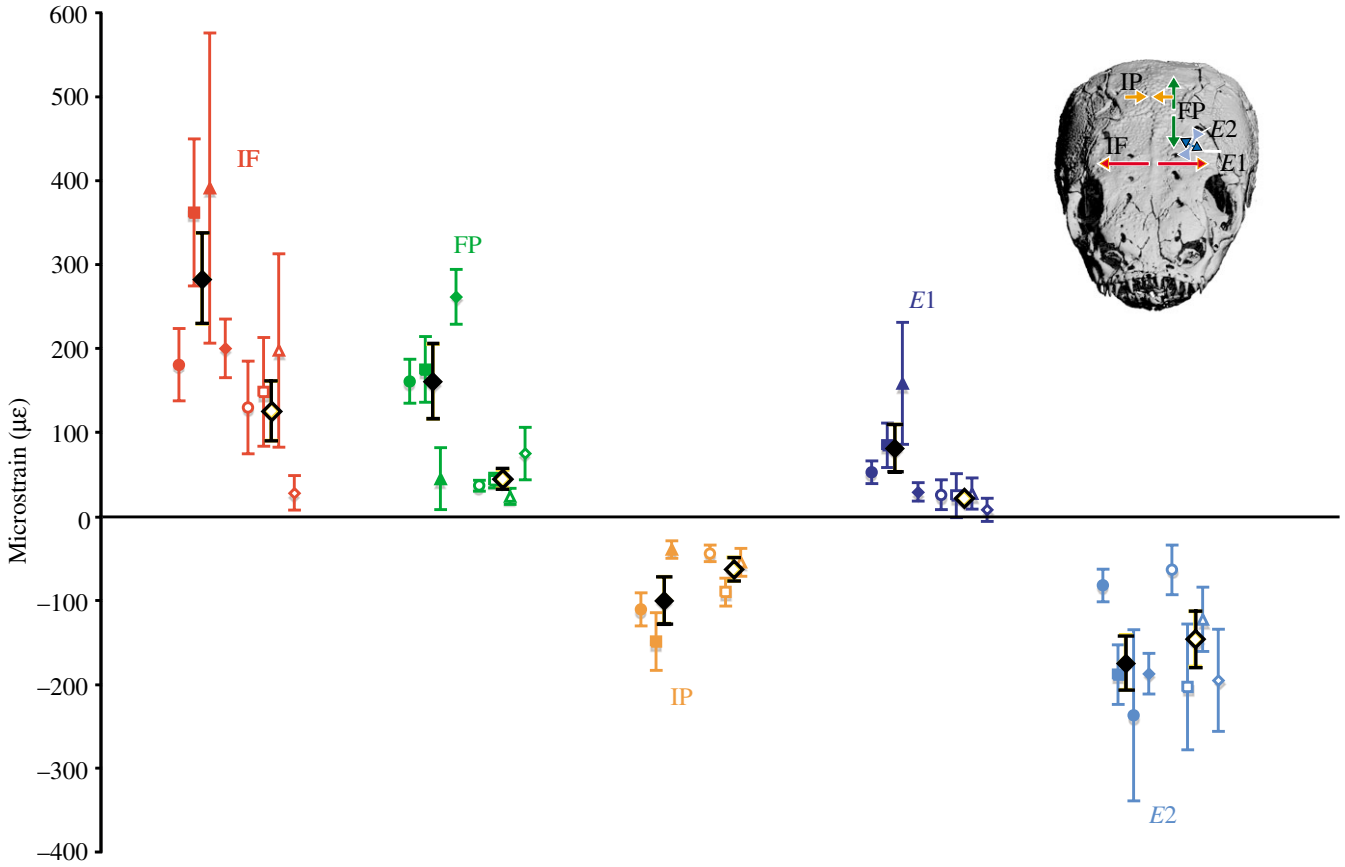

Fig. 4. Mean peak strains across the interfrontal (IF), interparietal (IP) and frontoparietal (FP) sutures, and maximum ($E1$) and minimum ($E2$) principal bone strains during suction and biting. Values are means ± 1 s.e.m. Filled symbols are strains measured in suction, and open symbols represent strains measured during biting. (circles, *Polypterus* 1; squares, *Polypterus* 2, triangles; *Polypterus* 3, diamonds; *Polypterus* 4). Black symbols are the mean of means for all four fish (± 1 s.e.m.). The most common strain pattern during suction is shown (inset). Mean peak IF, FP and IP strains are higher during suction than during biting. In addition, $E1$ is larger during suction than in biting, but there is no difference in the $E2$ in suction and biting.

suture and bone peak strains occurred at essentially the same time in the feeding cycle during suction ($P>0.05$ for all comparisons of timing of IP, FP, IF, *E*1 and *E*2; see Table 3 for mean timing ± s.d.). However, slight temporal differences between the strain peaks suggest that suction feeding deformed the posterior region of the skull first, and the 'wave' of deformation progressed anteriorly (see Fig. 5 for mean timing of peak strains and kinematics).

Biting

Kinematics

During biting events, maximum gape occurred at 45±7% (mean ± s.d., $N=4$) of the gape cycle, similar to when it was observed in suction feeding (*t*-test; $P=0.50$). Biting was also characterized by a shallower head lifting angle (–1.2±5.9°; mean ± s.d.; $N=4$) than suction (see Fig. 6). Although this low head lifting angle was not significantly different from values measured during suction (*t*-test; $P=0.188$), this result is consistent with Lauder's observation (Lauder, 1980) that the epaxial muscles are typically not activated during mastication. In addition, typical high-speed video of biting events demonstrates that, regardless of the absolute amount of head lifting, biting events lack the distinct peaks of head lifting that characterize suction (compare Figs 1 and 6).

The hyoid apparatus is adducted and generally did not change position during biting events (amount of hyoid depression=1.9±0.6 mm; mean ± s.d., $N=4$). The amount of hyoid depression during suction and biting was significantly different (*t*-test; $P=0.014$), which is clearly supported by the graphs of hyoid position provided in Figs 1 and 6.

Table 3. *Peak suture and bone strains during suction and biting, and the times at which they occur*

	Peak strain (με)	Timing (% gape cycle)	*N*
IP†			
Suction	–100±56	44±10	3
Biting	–63±24	53±14	3
FP			
Suction	161±89	47±19	4
Biting	45±22	62±4	4
IF			
Suction	284±108	60±18	4
Biting	126±71	61±26	4
*E*1 (tension)			
Suction	81±56	51±20	4
Biting	22±9	72±13	4
*E*2 (compression)			
Suction	–174±65	66±20	4
Biting	–146±66	73±8	4

Values are means ± s.d.; $N=3$ or 4.

†IP gauge detached during data collection in one individual (fish no. 4).

με, microstrain (strain$\times 10^{-6}$).

IP, interparietal; FP, frontoparietal; IF, interfrontal; *E*1, maximum principal bone strain; *E*2, minimum principal bone strain.

Head lifting and hyoid depression amounts during mastication (P) and oral jaw biting (B) were very similar (*t*-tests; head lifting, $P=0.377$; hyoid depression, $P=0.134$); however, maximum gape was significantly larger during oral jaw biting than in 'processing bites' (*t*-test; $P=0.002$). This difference in gape was not surprising given that 'processing bites' are defined as biting events in which the prey item is entirely within the mouth, allowing the jaws to close completely. (During oral jaw biting, the prey item frequently protrudes slightly from the mouth, which does not permit the jaws to fully close.) Based on the overall similarity of oral jaw biting (B) and 'processing bites' (P), both are simply termed biting events in the remainder of this paper.

In many of the biting events described here, a small amount of lateral head motion occurred (feeding events with large amounts of lateral head motion were not included in this study). However, the amount of lateral head motion was not quantified in this analysis because all video recordings were collected in lateral view.

Strain patterns

Biting on a prey item and mastication resulted in much more variable strain patterns than suction feeding (see Table 1). Although approximately 50% of biting events were characterized by four suture strain patterns, a total of 10 unique strain patterns were observed during oral jaw biting and mastication. The four most common patterns are shown in Fig. 3.

In spite of this variation, generalizations can be made about the strain types experienced by each suture individually during biting (Table 2). In 50% of biting events, the IP suture was loaded solely in compression; in an additional 43% of events, the IP experienced compression followed by tension (Table 2; see Fig. 6). However, the shift from compression to tension on the IP was observed in just one individual (fish no. 1) (see Table 1), and was exhibited only during mastication and not during prey manipulation. Therefore, this shift in strain polarity may not be typical for the IP suture in all biting events. The IF suture was loaded in tension during 71% of biting events, while the FP was loaded solely in tension 43% of the time but experienced solely compression in 29% of prey manipulation or mastication efforts (see Table 2).

Multiple strain peaks were observed in 50% of biting events. Although the primary peak typically occurs at or shortly after maximum gape, there was no clear connection between the secondary peaks and the kinematic measurements presented here (see secondary tension peaks in Fig. 6).

Strain magnitudes

Peak strains measured during biting at the IF, IP and FP sutures and within the frontal bone did not vary significantly across individual fish (ANOVA; IF, $P=0.547$; FP, $P=0.134$; IP, $P=0.108$; *E*1, $P=0.920$; *E*2, $P=0.231$).

During biting, the IF suture experienced higher strain

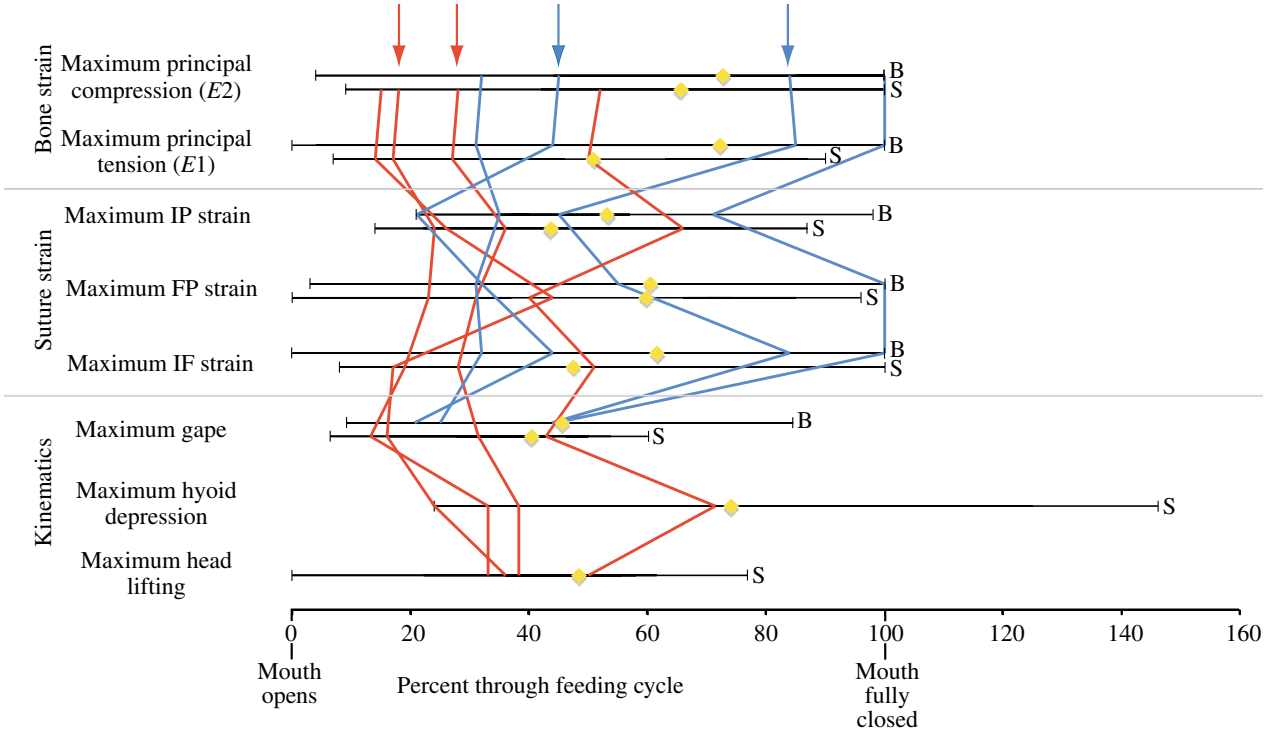

Fig. 5. Wide range of times at which peak suture and bone strains, and maximum gape, hyoid depression and head lifting, are achieved during biting (B) and suction (S) for all 52 feeding events included in this analysis. Peak hyoid depression and head lifting are given for suction only, because biting events do not exhibit distinct maxima of these variables. Mean timing values for each strain and kinematic peak are shown in yellow (mean ± s.d., N=4). For 8 individual trials, vertical paths show the times at which each strain and kinematic maximum were achieved. The red arrows indicate the first (left) and second (right) suction feeding events shown in Fig. 2. The blue arrows indicate the first (left) and second (right) biting events illustrated in Fig. 6. There was substantial variation in these timings between trials; however, the correlations between strain peak timing and the fish's kinematic activity were significant. If the temporal pattern of maximum strains and kinematics were identical in all suction or biting trials, then the vertical paths would all be parallel and located in the same region of the gape cycle, which they are not. Note that portions of the lines that represent suction events tend to track each other closely, as do portions of the biting events. This illustrates our finding that biting and suction events cause maximum skull and suture deformation at different points in the feeding cycle.

(126±71 με) (mean ± s.d.) than the FP suture (45±22 με), but this difference in magnitude was not significant (t-test; P=0.177; N=4). The IP suture experienced a smaller peak strain (–63±24 με) (mean ± s.d.) than both the FP and IF sutures; however, these differences were not significant (t-tests; IF>|IP|, P=0.062; FP>|IP|, P=0.134; N=3 for each). These differences in strain magnitude during biting are shown in Fig. 4 (open symbols).

In addition, comparison of peak IF strain with maximum strain measured by the E_c rosette component showed that biting caused larger deformation at the IF suture than within the frontal bone (t-test; P=0.027; IF=126±71 με; E_c=–3±13 με). Similarly, maximum strain across the FP suture (45±22 με; mean ± s.d.) was significantly greater than strain within the frontal bone at the same orientation (E_a=–29±24 με) (t-test; P=0.044).

The orientation of maximum principal strain (tension) during biting (ϕ=58±19° to the long axis of the frontal bone; Fig. 3) did not differ significantly from its mean position in suction (t-test; P=0.428).

Timing of strain peaks

Initially, no significant inter-individual variation was found in the times at which peak strains occurred during biting (MANOVA; P=0.258). However, closer examination of the data revealed that the times at which maximum IF strain and maximum (tension) principal strain within the left frontal bone occurred were different in at least one fish (ANOVA; P=0.036). In spite of this, paired t-tests of the timing of maximum suture and bone strains in all individuals demonstrated that, in all fish, mean peak suture (Fig. 6) and bone strains were achieved simultaneously in the feeding cycle, at or near maximum gape (P>0.05 for paired t-tests comparing timing of maximum IP, FP and IF sutures, and E1 and E2).

Although differences in the timing of maximum suture and bone strains during biting were not significant, the data show that the IP suture deformed first, followed by the IF and FP sutures that experienced peak strain nearly simultaneously. Finally, the frontal bone experienced maximum strain later in the feeding cycle (see Table 3 for means ± s.d.; Fig. 5).

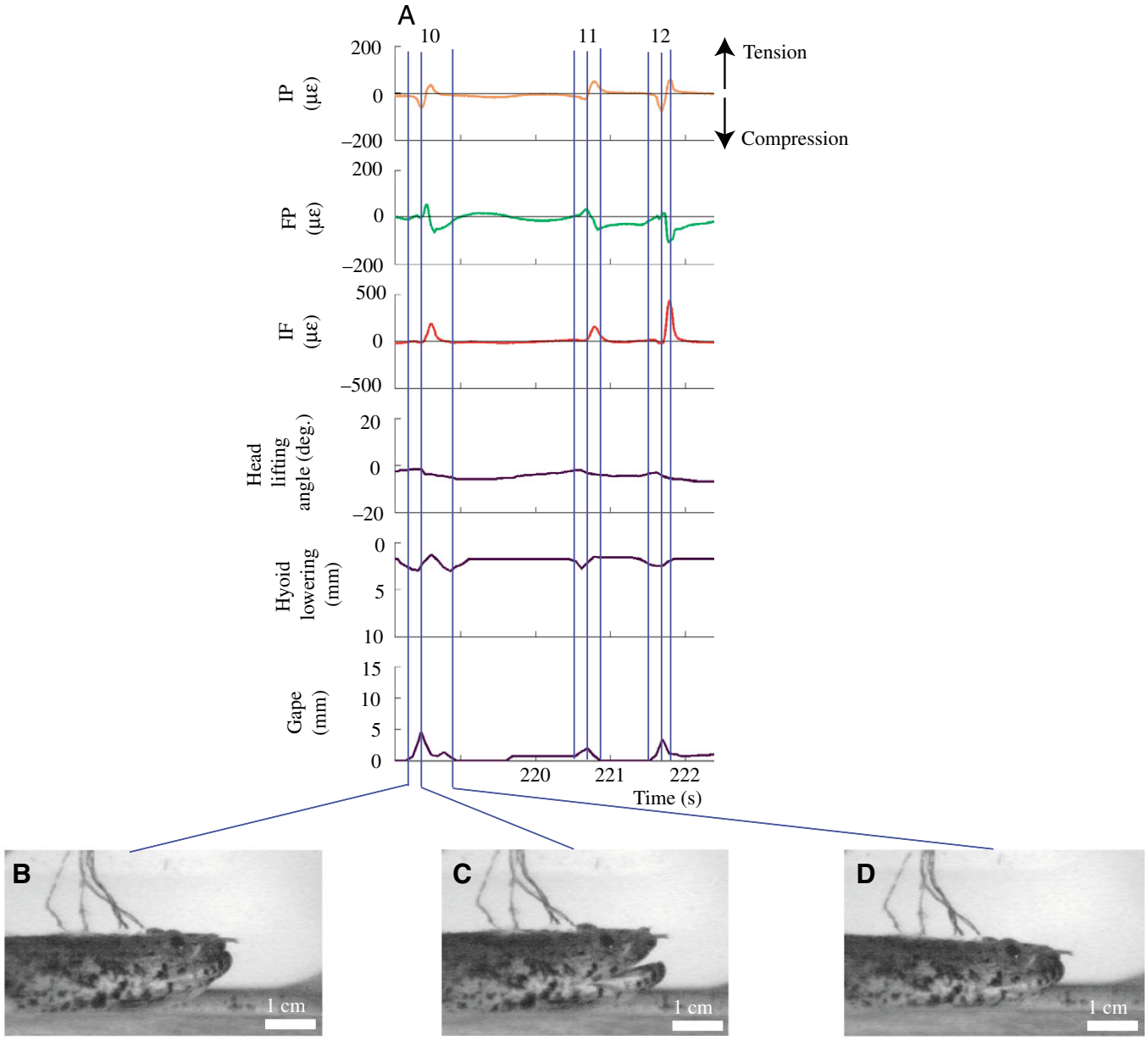

Fig. 6. (A) Kinematic measurements and suture strains during three biting events (*Polypterus* 1, trial 3, events 10–12; see Table S1 in supplementary material). Still frames of (B) mouth opening, (C) maximum gape and (D) mouth closing are given for the first biting event. The blue vertical lines indicate timing of the gape cycle. Strains due to biting were much more variable that strains caused by suction, so this particular trace should not be considered representative of all the strain traces measured during biting. In this particular event, the interparietal (IP) and frontoparietal (FP) sutures experience shifts in strain polarity, while the interfrontal (IF) suture is consistently loaded in tension. Note that the angle of head lifting and the amount of hyoid depression do not change appreciably in these events, in contrast to suction feeding.

Comparison of strain magnitudes during suction and biting

Peak suture and bone strains were smaller during biting than during suction (Fig. 4), but some of this difference can be attributed to intraspecific variation (MANOVA, P=0.000). However, this analysis also revealed that, for at least some of the suture and bone strains, the difference in strain magnitude between suction and biting occurred in at least one fish (MANOVA, P=0.000). Specifically, the FP, IP and IF sutures experienced significantly less deformation during biting than in suction (MANOVA, ANOVA; see Table 3 for means ± s.d. and Table 4 for P-values). In addition, the maximum (tensile) principal strain was smaller during biting than suction (Table 4; MANOVA, P=0.007); however, the minimum (compressive) principal strain was the same in suction and biting (see Tables 3 and 4). Therefore, all three sutures analyzed here experienced significantly greater deformation than the frontal bone during suction than during biting.

Comparison of strain peak timing during suction and biting

Most peak suture and bone strains occurred at the same times in the feeding cycle in both suction and biting (MANOVA; P=0.058). Specifically, the timing of maximum strain across the IF and IP sutures and the minimum (compressive) principal strain did not vary significantly between suction and biting (MANOVA; P>0.05 for each; Table 4). However, maximum FP strain and maximum (tensile) principal strain occurred significantly later during biting (MANOVA; FP, P=0.04; E1, P=0.007). These differences in FP and E1 strain peak timing are shown graphically in Fig. 5.

Table 4. *Results of MANOVA to determine whether there are differences in peak strains or the times at which they occur across fish or between feeding types (suction or biting)*

	P	
	Peak strain	Timing
Fish		
IP	0.016*	0.093
FP	0.000*	0.163
IF	0.173	0.074
E1 (tension)	0.106	0.014*
E2 (compression)	0.068	0.072
Feeding mode†		
IP	0.046*	0.252
FP	0.000*	0.040*
IF	0.016*	0.931
E1 (tension)	0.007*	0.007*
E2 (compression)	0.465	0.408

'Fish number' and 'feeding mode' were considered independent variables, while the magnitude and timing of peak IP, FP, IF suture strain and maximum (tensile) and minimum (compressive) principal bone strains were dependent variables.

IP, interparietal; FP, frontoparietal; IF, interfrontal; E1, maximum principal bone strain; E2, minimum principal bone strain.

†Feeding mode means suction or biting.

*Difference is significant at the P<0.05 level.

Correlating timing of strain peaks with kinematics

During suction, the occurrence of peak suture and bone strains was significantly correlated with maximum gape (P<0.05 for timing of IP, FP, IF, E1 and E2; see Table 5 for partial correlation coefficients), which was expected based on the strains and kinematic data shown in Fig. 2. In addition, the timing of peak IP and FP suture strains, and the timing of maximum and minimum principal strains within the left frontal bone, were significantly correlated with the time that maximum head lifting and hyoid lowering occurred (P<0.05; Table 5). In contrast, maximum IF strain did not coincide with maximum head lifting or hyoid lowering during suction (see Table 5).

During biting, the occurrence of maximum gape was correlated with the times at which maximum FP and IP strains were recorded (P<0.05 for both; see Table 5 for partial correlation coefficients). However, the occurrence of maximum (E1) and minimum (E2) principal bone strains was not correlated with maximum gape in biting events.

Although these correlations between strain peak timing and the fish's kinematic activity were significant, there was substantial variation in these variables among trials (see Fig. 5). If the temporal pattern of maximum strains, and

Table 5. *Partial correlation matrix for timing of kinematic variables and the timing of maximum suture and bone strains during suction and biting*

	Maximum gape	Head lifting	Hyoid depression	IP	FP	IF	E1 (tension)	E2 (compression)
Maximum gape								
Head lifting	0.548							
Hyoid depression	0.477 —							
IP	0.851 0.649	0.576 —	0.516					
FP	0.529 0.469	0.457 —	0.549 —	0.769				
IF	0.485	—		0.696 0.692				
E1 (tension)	0.707	0.626	0.351	0.731	0.689	0.648 0.402		
E2 (compression)	0.449	0.344	0.36	0.687		0.889 0.415	0.714 0.511	

Only correlations significant at the 0.05 level are shown. Correlations during suction are shown in the top of each cell; correlations during biting are shown at the bottom of each cell. Dashes indicate correlations that, although they can be calculated, are not meaningful because there are no appreciable peaks in head lifting or hyoid depression during biting.

IP, interparietal; FP, frontoparietal; IF, interfrontal; E1, maximum principal bone strain; E2, minimum principal bone strain.

maximum gape, head lifting, and hyoid depression were identical in all suction or biting trials, then the vertical lines shown in Fig. 5 would all be parallel and located in the same region of the gape cycle, which they are not. However, the lines that represent suction events tend to track each other closely, while biting events are also self-similar (but note the biting event on the far left). This supports our finding that biting and suction events cause maximum skull and suture deformation at different points in the feeding cycle.

MicroCT scans of experimental specimens

Dramatic differences in the cross-sectional morphology of the IF, FP and IP sutures were easily identified from the microCT scans of the experimental specimens (Fig. 7). At the position of the IF gauge, the IF suture exhibited an abutting morphology; that is, it lacked interdigitation. The left and right frontal bones were therefore fairly flat-edged at their contact in the midline of the skull. The IP suture, however, was greatly interdigitated in cross-section, and the degree of interdigitation increased along its length from anterior to posterior. At the position of the IP gauge, the IP suture had not reached its maximum amount of interdigitation. The FP suture exhibited a highly overlapping morphology with very small interdigitations.

Interestingly, the IF, FP and IP sutures appeared identical in dorsal view (see Figs 1 and 7).

Discussion

Although the overall strain patterns observed on the skull during suction and biting are different (Fig. 3), and suction strains exceed biting strains (Fig. 4), each suture experiences a characteristic strain polarity (Table 2). Specifically, the IF is tensed, while the IP is compressed, regardless of whether the fish is sucking the prey item into the buccal cavity or biting on it. The FP suture, however, experiences variable strain patterns – tension or compression or a shift from one to the other – within and among feeding events (Fig. 3).

Suture and bone strains are generally larger during suction than during biting, but not all of these differences in magnitude are significant (Table 4). In addition, all sutures experienced greater deformation than the frontal bone in both feeding types, but this difference was more pronounced in suction feeding. During suction, peak suture and bone strains occur simultaneously at maximum gape, but during biting, peak IF and the maximum principal tension occur after maximum gape.

Partial correlations between the timing of strain peaks and maximum gape, maximum hyoid lowering, and peak head lifting do not reveal which of these kinematic variables plays the largest role in deforming the skull during suction.

Correlating suture morphology and function

Several experiments report a correlation between sutural interdigitation and compression in miniature pigs (Herring and Mucci, 1991; Rafferty and Herring, 1999; Herring and Teng, 2000). In addition, sutures that are flat-edged in cross section are loaded in tension (Herring and Teng, 2000; Sun et al., 2004). These correlations are maintained even when the prevailing loading conditions on a suture change during ontogeny. For example, in 3-month-old miniature pigs the posterior interfrontal suture is compressed during chewing, and exhibits a highly interdigitating morphology. By 7 months of age, however, the posterior interfrontal suture is loaded less in compression and more in tension, which is reflected by a loss of interdigitation in the ectocranial portion of the suture resulting in an abutting morphology (Sun et al., 2004).

In this study, the highly interdigitated IP suture is typically loaded in compression during both suction and biting (Tables 1 and 2; Fig. 3), although strains measured during suction were significantly higher than during biting (Tables 3 and 4; Fig. 4). The IF suture, which exhibits an abutting morphology, is loaded in tension in the majority of suction and biting events reported here (Tables 1 and 2). The FP suture is highly overlapping in cross section, and lacks the well-defined interdigitations that characterize the IP suture. Much more variable strains were measured at the FP suture than at the IF and IP sutures, including shifts in strain polarity within a single feeding event (Tables 1 and 2). It is possible that the overlapping morphology of the FP suture represents a morphological compromise, based upon the tensile and compressive strains to which it is subjected.

The relationships between suture form and function reported here have important implications for using suture shape to infer skull function in fossil fish and amphibians. This study demonstrates that the relationships between compression and interdigitation, and relatively flat sutures and tension, hold even when the sources of strains – in this case, the muscles that act during feeding – are unclear. In addition, these correlations can be used to reconstruct how the skull deforms as a unit (see below) in fossil as well as extant taxa.

More fundamentally, these data demonstrate that fish sutures, at least in *Polypterus*, are similar to sutures in mammals, in that interdigitation is associated with compression, and abutting sutures are loaded in tension. Clearly, the taxonomic distance between these groups implies that these correlations between suture form and function are widespread among vertebrates, and can be applied to aquatic as well as terrestrial vertebrates. In addition, the presence of very similar suture morphologies in such different species as miniature pigs and *Polypterus* suggests that suture morphology is highly conserved in vertebrates. Therefore, questions about the function of unusual suture morphologies, such as those seen in amphisbaenids (Gans, 1960), and about how these uniquely shaped sutures originated, can now be placed in the wider context of what suture shapes are ‘typical’ among vertebrates.

Deformation of the skull as a unit in Polypterus

Our results show that the anterior part of the skull is pulled apart, while the posterior region of the skull (in the vicinity of the parietals) is compressed during suction and biting feeding behavior in *Polypterus* (Fig. 3). Therefore, at the front of the

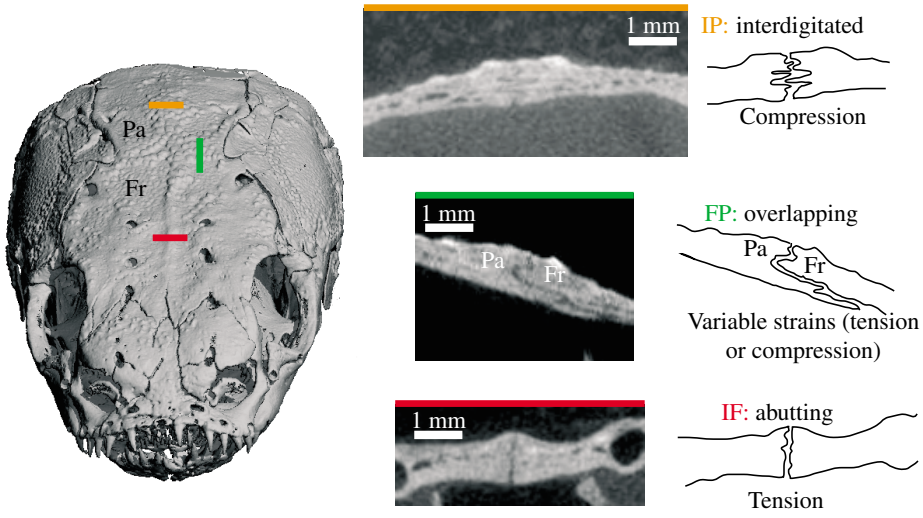

Fig. 7. Correlating suture shape and function in *Polypterus* using microCT slices. Line drawings of each suture are provided to the right of the actual slice images. The interparietal (IP) suture, which is loaded in compression during suction and biting, is highly interdigitated in cross section. In contrast, the interfrontal (IF) suture has an abutting (i.e. flat-edged) morphology and is typically loaded in tension during suction and biting. The frontoparietal (FP) suture, however, is highly overlapping, and is loaded in tension or compression, and may experience a shift in strain polarity during suction and biting. Pa, parietal; Fr, frontal.

skull the right and left halves of the skull rotate laterally, away from one another, during normal feeding. This pattern of skull deformation is the opposite of what is observed in miniature pigs; that is, compression has been measured at the front of the skull (internasal suture), coupled with tension more posteriorly (across the IF and IP sutures) in pigs during normal chewing (Sun et al., 2004).

This combination of tension at the interfrontal and compression at the interparietal implies that the axis of rotation for the two halves must be located in the midline of the skull, between the IF and IP gauges. Based on the dramatic change in the morphology of the IP suture from low to high interdigitation along its length antero-posteriorly, it is reasonable to suppose that the fulcrum of the skull roof is located near the anterior portion of the IP suture. The interfrontal suture does not exhibit a comparable shape change at any point along its length.

The overall strain environment described above, combined with the change in morphology along the IP suture, suggests an explanation for some of the more unusual strain patterns recorded in this study. In fish no. 1 only, a transition from compression to tension was observed across the IP suture during mastication (see Table 1). This shift in strain polarity may simply be due to the fish behaving differently in that event, in a manner that is not apparent from the high-speed videos. However, it is also possible that this shift reflects the proximity of the IP gauge to the axis of rotation in this particular individual, similar to observations made by others (Sun et al., 2004). If this is the case, then the strain patterns reported for any suture will be highly sensitive to the location of the strain gauge, and great care must be taken with strain gauge positioning when performing replicate experiments.

Possible explanations for the observed suture and bone strain patterns

The strain data presented here show that suture and bone strains in the skull of *Polypterus* are zero when the fish is resting or swimming, and that the strains are correlated with the action of feeding. In addition, we found that peak strains due to both suction and biting occur at or shortly after maximum gape, well before the teeth contact the prey item. Based on these observations, it is reasonable to conclude that the bone and suture strains measured here result from muscle contraction during feeding. This conclusion agrees well with studies of suture function in miniature pigs, which show that muscle contraction during mastication, assessed using electromyography, causes deformation of skull roof sutures (Herring and Mucci, 1991; Herring and Teng, 2000; Sun et al., 2004). In fact, the magnitude and pattern of these suture strains were replicated by muscle stimulation in unconscious pigs, even when the lower and upper teeth were not in occlusion (Herring and Mucci, 1991; Herring and Teng, 2000), suggesting that the act of biting on a food item produces negligible strain in the skull roof.

In this study, muscle activity patterns were not measured, so a direct correlation between muscle action, and suture and bone strains, cannot be made. However, using our measurements of the feeding kinematics of *Polypterus*, observations of skull and muscle anatomy made on our specimens and from the literature (Lauder, 1980; Allis, 1922), as well as muscle activity patterns recorded during feeding in *Polypterus* (Lauder, 1980), we provide preliminary evaluation of the following hypotheses to explain the suture and bone strains measured in this study. However, it should be noted that the substantial variation in the timing of peak bone and suture strains in this study suggests that the timing of muscle activity also varied widely between trials; therefore, Lauder's descriptions (Lauder, 1980) of when particular muscles are used in the feeding cycle may not capture the range of behaviors seen in this study. In addition, our efforts here to link muscle activity patterns from the literature to our bone and suture strain data only consider the effect of each muscle independently. In reality, much overlap in the timing of muscle activation occurs, the details of which depend on the speed of the feeding cycle (Lauder, 1980) among other variables.

Based on its position (Fig. 8) and timing of activity (Lauder,

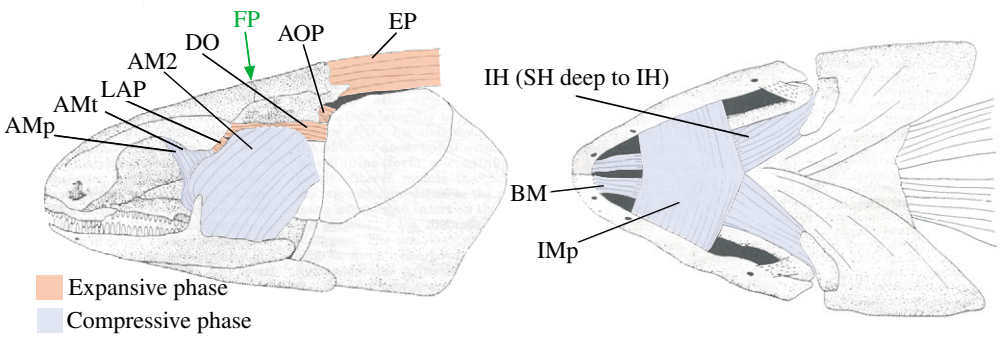

Fig. 8. Dissection of *Polypterus* in lateral and ventral views, showing many of the muscles that act during the expansive and compressive phases of feeding. Expansive phase muscles are shown in pink, while compressive phase muscles are shown in blue. The position of the frontoparietal (FP) suture is indicated by the green arrow. Modified from Lauder (Lauder, 1980), with permission of the author. AMp, adductor mandibulae pterygoideus; AMt, adductor mandibulae temporalis; LAP, levator arcus palatini; AM2, adductor mandibulae, division 2; DO, dilator operculi; AOP, adductor operculi; EP, epaxialis; IH, interhyoideus; SH, sternohyoideus; BM, branchiomandibularis; IMp, intermandibularis posterior.

1980), it is likely that the levator arcus palatini (LAP) contributed to the tension measured across the IF suture at maximum gape in both suction and biting. However, the effect of the LAP on the FP and IP sutures is unclear. In addition, contraction of the LAP might be the cause of the tension measured within the left frontal bone at a posterolateral angle to the IF suture. However, the maximum principal tension actually recorded on the left frontal bone was oriented anterolaterally (approximately 60° from the long axis of the left frontal bone), so the LAP alone cannot account for the measured strains.

The adductor hyomandibulae (AHY), which originates on the opisthotic and inserts on the medial surface of the hyomandibula (not shown in Fig. 8; but is continuous with the figured adductor operculi, AOP) (Allis, 1922; Lauder, 1980), is the only muscle we can identify that might cause compression at the IP suture. Specifically, we hypothesize that contraction of the AHY may pull the head of the hyomandibula medially into its fossa on the neurocranium, resulting in compression in the neurocranium and at the IP suture. Based on its position, it is unlikely that the AHY contributed to deformation of the frontal bones.

The epaxial (EP) muscles insert on the posterior margin of the neurocranium (Fig. 8), including the posterior edges of the parietals (Allis, 1922). Therefore, contraction of the EP muscles could result in tensile strains across the FP suture. Because the EP muscles are active in the expansive phase of suction, but not in biting, this tension at the FP would be observed only during suction. However, during suction the EP muscles are active well before maximum gape (Lauder, 1980); therefore, some other muscle or set of muscles must primarily cause the tensile peak in FP strain that coincides with maximum gape. Finally, the lack of a direct connection between the frontal bones and the EP suggests that this muscle did not make an important contribution to the principal strains measured in the left frontal bone.

Contraction of the dilator operculi (DO) (Allis, 1922; Lauder, 1980) could pull the postfrontal and frontal posterolaterally, causing tension at the IF suture, and compression at the FP suture (see Fig. 8). The DO is active during both suction and biting, close to when maximum gape is achieved (Lauder, 1980). In addition, contraction of the DO would be expected to stretch the left frontal bone posterolaterally; however, the anterolateral orientation of tension within the left frontal bone that we measured (see Fig. 3) is not consistent with this hypothesis.

The sternohyoideus (SH) muscle aids in hyoid depression, an important part of the expansive phase of suction feeding; however, its distant location from the skull roof (see Fig. 8) argues against its being a prime cause of the suture and bone strains reported here. In addition, mastication in *Polypterus* is distinguished by high-level activity in the branchiomandibularis (BM), intermandibularis posterior (IMp) and interhyoideus (IH) (Lauder, 1980). However, the distance between the insertion points of these muscles and the implanted strain gauges argues against their influencing deformation in the skull roof during biting (see Fig. 8).

The adductor mandibulae (division 2) (AM2), adductor mandibulae ‘temporalis’ (AMt), and adductor mandibulae ‘pterygoideus’ (AMp) muscles (Fig. 8) are activated during the compressive phase of suction and biting. Because the AM2 does not directly insert on the skull roof (Allis, 1922; Lauder, 1980), its effect on the sutures analyzed here is difficult to anticipate. However, the origin and insertion points of the AMt and AMp, and when they are activated in the feeding cycle, (Lauder, 1980) suggest that they could strongly influence deformation at the IF suture. The effect of the adductor complex on the FP suture is difficult to anticipate; however, contraction of AMt and AMp may slightly displace the frontals laterally with respect to the parietals. This lateral shearing motion would produce a tensile component, as measured by a single-element strain gauge spanning the FP suture. Finally, contraction of the adductor complex muscles is probably the primary cause of the measured deformation of the frontal bone

(see Fig. 3). Specifically, the AM2 may cause compression of the left frontal along its long axis, which is roughly consistent with the observed orientation of the minimum principal strain (*E*2) (Fig. 3). While the measured maximum principal strain (*E*1) was oriented approximately 60° from the long axis of the left frontal bone, the origin and insertion points of AMt and AMp (Fig. 8) suggest that these muscles would cause tension within the frontal bone perpendicular to the IF suture.

We must emphasize that these hypotheses linking suture and bone strain to muscle activity cannot be tested using the data we present here. These hypotheses could be tested using electromyography or sonomicrometry.

Conclusions

The sutures and bones in the skull of *Polypterus* are deformed similarly during suction and biting; however, suction results in larger strains than biting, which was unexpected. Specifically, the IF suture is tensed, while the IP suture is compressed; the FP suture experiences variable strains. During both suction and biting, IF strain exceeded FP strain, and both were greater than IP strains. In addition, tensile strains at the FP and IF sutures exceeded strains measured within the left frontal bone. All suture and bone strains reach their peak shortly after maximum gape; therefore, these strains are probably a consequence of muscle contraction and not indirect loading due to biting on a prey item.

High-resolution CT scans of the experimental specimens reveal that the IF, IP and FP sutures exhibit very different morphologies in cross-section, even though they appear similar in dorsal view. The fact that the IF and IP sutures experience a characteristic strain type suggests a tight link between suture form and function in *Polypterus*. The compressed IP is highly interdigitated, while the tensed IF is comparatively flat in cross-section. The FP suture has an overlapping morphology, which may be a response to the varying strains experienced by this suture. These relationships between suture form and function are apparent even though the cause of the strains measured here was not directly established.

The fact that compression is associated with interdigitated sutures, and tension with flat-edged (abutting) sutures in *Polypterus* as well as in miniature pigs, implies that these correlations between suture form and function may be widespread among vertebrates, and can be used to infer skull deformation patterns in extinct taxa.

Based on these strain data, each half of the skull in *Polypterus* probably rotates laterally during suction feeding and biting on a prey item, with tension at the front of the skull and compression posteriorly. This rotation suggests that measured strains across cranial sutures will vary greatly depending on gauge location, and care must be taken to ensure that replicate experiments focus on the same portion of the sutures of interest.

Finally, we propose that the location of the LAP, DO and AM complex muscles in the skull, and the times at which they are active during the feeding cycle, suggest that they may be responsible for producing tension in the IF suture during suction and biting. The EP muscles, judging from their position, probably load the FP in tension during suction but not biting. The AHY muscle may load the IP in compression, but its effect is unclear given its early recruitment in the feeding cycle. The AM complex muscles likely produce tension across the IF suture at maximum gape, and may also stretch the FP suture. In addition, the AM complex probably has the strongest influence on the magnitude and direction of the principal strains measured within the left frontal bone. However, these hypotheses linking muscle action to the bone and suture strains measured in this study should be assessed in future work using electromyography or sonomicrometry.

List of abbreviations

ϕ	orientation of *E*1 relative to E_a
AHY	adductor hyomandibulae
AM2	adductor mandibulae (division 2)
AMp	adductor mandibulae ‘pterygoideus’
AMt	adductor mandibulae ‘temporalis’
AOP	adductor operculi
B	biting
BM	branchiomandibularis
DO	dilator operculi
*E*1	maximum tensile principal strain
*E*2	minimum compressive principal strain
EP	epaxial
FP	frontoparietal
IF	interfrontal
IH	interhyoideus
IMp	intermandibularis posterior
IP	interparietal
LAP	levator arcus palatini
MicroCT	micro-computed tomography
P	processing bite
S	suction
SB	suction plus biting
SH	sternohyoideus

We would like to thank Pedro Ramirez for animal care, Eric Tytell for surgery advice and assistance, Andrew Biewener and Farish A. Jenkins, Jr for sponsoring this research, and George V. Lauder and Andrew H. Knoll for help and comments during the writing of this manuscript. We also thank Roberto Fajardo for generating the 3D images used in Fig. 3. Finally, we thank the two anonymous reviewers for their advice and recommendations that improved this manuscript.

References

Alfaro, M. E., Janovetz, J. and Westneat, M. W. (2001). Motor control across trophic strategies: muscle activity of biting and suction feeding fishes. *Am. Zool.* **41**, 1266-1279.

Allis, E. P. (1922). On the cranial anatomy of *Polypterus*, with special reference to *Polypterus bichir*. *J. Anat.* **56**, 189-292.

Bartsch, P. (1997). Aspects of craniogenesis and evolutionary biology in polypteriform fishes. *Neth. J. Zool.* **47**, 365-381.

Beaumont, E. I. (1977). Cranial morphology of the Loxommatidae (Amphibia: Labyrinthodontia). *Philos. Trans. R. Soc. Lond. B. Biol. Sci.* **280**, 29-101.

Behrents, R. G., Carlson, D. S. and Abdelnour, T. (1978). *In vivo* analysis of bone strain about the sagittal suture in *Macaca mulatta* during masticatory movements. *J. Dent. Res.* **57**, 904-908.

Bourbon, B. M. (1982). Deformation of cranial sutures during masticatory activity: a strain gauge application. PhD dissertation, University of Pennsylvania, USA.

Carroll, R. L. (1988). *Vertebrate Palaeontology and Evolution*, 698 pp. New York: W. H. Freeman.

Clack, J. A. (2002). The dermal skull roof of *Acanthostega gunnari*, an early tetrapod from the Late Devonian. *Trans. R. Soc. Edinb. Earth Sci.* **93**, 17-33.

Clack, J. A. (2003). *Gaining Ground: The Origin and Evolution of Tetrapods*, 369 pp. Bloomington, IN: Indiana University Press.

Ferry-Graham, L. A. and Lauder, G. V. (2001). Aquatic prey capture in ray-finned fishes: a century of progress and new directions. *J. Morphol.* **248**, 99-119.

Gans, C. (1960). Studies on amphisbaenids (Amphisbaenia, Reptilia). 1. A taxonomic revision of the Trogonophinae and a functional interpretation of the amphisbaenid adaptive pattern. *Bull. Am. Mus. Nat. Hist.* **119**, 129-203.

Gerking, S. D. (1994). *Feeding Ecology of Fish*, 416 pp. San Diego: Academic Press.

Grubich, J. R. (2001). Prey capture in actinopterygian fishes: a review of suction feeding motor patterns with new evidence from an elopomorph fish, *Megalops atlanticus*. *Am. Zool.* **41**, 1258-1265.

Heckel, J. J. (1847). Ichthyologie (von Syrien). In *Reisen in Europa, Asien und Africa, mit besonderer Rücksicht auf die naturwissenschaftlichen Verhältnisse der betreffenden Länder unternommen in den Jahren 1835 bis 1841* v. 1 (pt 2) (ed. J. von Russegger), pp. 205-357. Stuttgart. Ichthyol. von Syrien.

Herring, S. W. and Mucci, R. J. (1991). *In vivo* strain in cranial sutures: the zygomatic arch. *J. Morphol.* **207**, 225-239.

Herring, S. W. and Ochareon, P. (2005). Bone – special problems of the craniofacial region. *Orthod. Craniofac. Res*. **8**, 174-182.

Herring, S. W. and Teng, S. (2000). Strain in the braincase and its sutures during function. *Am. J. Phys. Anthropol.* **112**, 575-593.

Janvier, P. (1996). *Early Vertebrates*: *Oxford Monographs on Geology and Geophysics*, No. 33. Oxford: Clarendon Press.

Jarvik, E. (1947). Notes on the pit-lines and dermal bones of the head in *Polypterus*. *Zool. Bidr. Upps.* **25**, 61-78.

Jaslow, C. R. and Biewener, A. A. (1995). Strain patterns in the horncores, cranial bones and sutures of goats (*Capra hircus*) during impact loading. *J. Zool.* **235**, 193-210.

Kathe, W. (1999). Comparative morphology and functional interpretation of the sutures in the dermal skull roof of temnospondyl amphibians. *Zool. J. Linn. Soc.* **126**, 1-39.

Lauder, G. V. (1980). Evolution of the feeding mechanism in primitive actinopterygian fishes: a functional anatomical analysis of *Polypterus*, *Lepisosteus*, and *Amia*. *J. Morphol.* **163**, 283-317.

Lauder, G. V. (1982). Structure and function in the tail of the Pumpkinseed sunfish (*Lepomis gibbosus*). *J. Zool.* **197**, 483-495.

Lauder, G. V. (1985). Aquatic feeding in lower vertebrates. In *Functional Vertebrate Morphology* (ed. M. Hildebrand, D. M. Bramble, K. F. Liem and D. B. Wake), pp. 210-229. Harvard: Harvard University Press.

Lauder, G. V. and Gillis, G. B. (1997). Origin of the amniote feeding mechanism: experimental analyses of outgroup clades. In *Amniote Origins: Completing the Transition to Land* (ed. S. Sumida and K. Martin), pp. 169-206. San Diego: Academic Press.

Lauder, G. V. and Lanyon, L. E. (1980). Functional anatomy of feeding in the bluegill sunfish *Lepomis macrochirus*: *in vivo* measurement of bone strain. *J. Exp. Biol.* **84**, 33-55.

Lauder, G. V. and Reilly, S. M. (1994). Amphibian feeding behavior: comparative biomechanics and evolution. In *Advances in Comparative and Environmental Physiology: Biomechanics of Feeding in Vertebrates* (ed. V. L. Bels, M. Chardon and P. Vandewalle), pp. 163-195. Berlin: Springer-Verlag.

Lieberman, D. E., Krovitz, G. E., Yates, F. W., Devlin, M. and St. Claire, M. (2004). Effects of food processing on masticatory strain and craniofacial growth in a retrognathic face. *J. Hum. Evol.* **46**, 655-677.

Liem, K. F. (1978). Modulatory multiplicity in the functional repertoire of the feeding mechanism in cichlid fishes. I. Piscivores. *J. Morphol.* **158**, 323-360.

Metzger, K. A. and Ross, C. F. (2004). *In vivo* loading patterns in the alligator mandible. *J. Morphol.* **260**, 313A.

Muller, M. and Osse, J. W. M. (1984). Hydrodynamics of suction feeding in fish. *Trans. Zool. Soc. Lond.* **37**, 51-135.

Noack, K., Zardoya, R. and Meyer, A. (1996). The complete mitochondrial DNA sequence of the bichir (*Polypterus ornatipinnis*), a basal ray-finned fish: Ancient establishment of the consensus vertebrate gene order. *Genetics* **144**, 1165-1180.

Ogle, R. C., Tholpady, S. S., McGlynn, K. A. and Ogle, R. A. (2004). Regulation of cranial suture morphogenesis. *Cells Tissues Organs* **176**, 54-66.

Rafferty, K. L. and Herring, S. W. (1999). Craniofacial sutures: morphology, growth, and *in vivo* masticatory strains. *J. Morphol.* **242**, 167-179.

Smith, K. K. and Hylander, W. L. (1985). Strain gauge measurement of mesokinetic movement in the lizard *Varanus exanthematicus*. *J. Exp. Biol.* **114**, 53-70.

Sun, Z., Lee, E. and Herring, S. W. (2004). Cranial sutures and bones: growth and fusion in relation to masticatory strain. *Anat. Rec. A Discov. Mol. Cell. Evol. Biol.* **276**, 150-161.

Thomason, J. J., Grovum, L. E., Deswysen, A. G. and Bignell. W. W. (2001). *In vivo* surface strain and stereology of the frontal and maxillary bones of sheep: implications for the structural design of the mammalian skull. *Anat. Rec.* **264**, 325-338.

Thomson, K. S. (1993). Segmentation, the adult skull, and the problem of homology. In *The Skull*, Vol. 2: *Patterns of Structural and Systematic Diversity* (ed. J. Hanken and B. K. Hall), pp. 36-68. Chicago: University of Chicago Press.

Thomson, K. S. (1995). Graphical analysis of dermal skull roof patterns. In *Functional Morphology in Vertebrate Paleontology* (ed. J. J. Thomason), pp. 193-204. Cambridge: Cambridge University Press.

Thomson, K. S. and Bossy, K. H. (1970). Adaptive trends and relationships in early Amphibia. *Forma et Functio* **3**, 7-31.

Venkatesh, B., Ning, Y. and Brenner, S. (1999). Late changes in spliceosomal introns define clades in vertebrate evolution. *Proc. Natl. Acad. Sci. USA* **96**, 10267-10271.

Westneat, M. W. (1990). Feeding mechanics of teleost fishes (Labridae: Perciformes): a test of four-bar linkage models. *J. Morphol.* **205**, 269-295.

Table S1. Peak bone and suture strains and the times at which they occur (expressed as percent of the feeding cycle), and kinematic measurements during suction and biting in *Polypterus*. Fish number, trial and event number, feeding type classification, and presence or absence of prey capture are noted for each event. S indicates suction events, while SB denotes "suction followed by biting". Analysis of the kinematic measurements during these events revealed that, within the limitations of this study, S and SB events should be considered identical. Therefore, both are referred to as simply suction feeding. B indicates an event in which the prey item is bitten, usually during manipulation, while P events are mastication, with the prey item fully in the fish's mouth. These two events are not distinguishable using our kinematic measurements; hence, both are termed "biting" in this paper.

Fish	Trial	Event	Classif.	Prey capture?	Event duration (s)	Min. IP strain (με)	Percent through event that Min. IP strain occurs	Max FP strain (με)	Percent through event that Max. FP strain occurs	Max IF strain (με)	Percent through event that Max. IF strain occurs	Max E1 (με)	φ†	Percent through event that Max. E1 occurs	Max E2 (με)	Percent through event that Max. E2 occurs
1	3	1	**S**	y	0.267	-80	36	100	31	160	28	59	60	27	-37	28
1	3	9	**S**	n	0.450	-53	46	48	48	-13	40	-9	19	92	-45	90
1	3	2	**SB**	n	0.250	-180	24	159	23	152	19	46	65	17	-59	18
1	3	3	**SB**	n	0.267	-181	31	150	29	201	24	78	65	23	-136	24
1	7	1	**SB**	y	0.133	-105	55	220	36	368	42	103	72	38	-64	43
1	9	1	**SB**	y	0.216	-67	50	207	47	238	100	64	84	100	-172	100
1	9	2	**SB**	n	0.216	-108	35	242	33	158	29	29	69	27	-62	28
2	2	1	**SB**	y	0.104	-196	77	221	72	462	70	120	66	69	-182	100
2	2	2	**SB**	n	0.264	-123	75	122	70	153	96	61	63	85	-165	85
2	6	1	**SB**	y	0.160	-214	14	228	9	471	8	160	65	7	-279	9
2	6	2	**SB**	n	0.104	-26	87	2	0	40	96	-25	58	46	-54	100
2	7	1	**SB**	y	0.144	-185	22	253	17	589	80	121	69	11	-289	78
2	8	1*	**SB**	y	0.150	-	-	225	37	457	41	73	68	40	-162	42
3	9	1*	**SB**	y	0.096	-	-	225	63	865	44	292	80	42	-389	44
3	1	1	**S**	n	0.200	-19	26	6	44	88	17	58	78	14	-52	15
3	1	2	**SB**	y	0.112	-68	66	23	40	206	51	129	77	50	-135	52
3	2	5	**SB**	n	0.248	-34	20	-10	10	50	50	13	55	16	-70	60
3	2	6	**SB**	n	0.184	-36	34	-12	20	73	83	8	59	29	-94	96
3	3	3*	**SB**	y	0.072	-	-	38	92	1066	59	451	81	56	-680	61
4	8	1*	**S**	y	0.104	-	-	200	96	86	88	11	75	84	-97	100
4	8	2*	**SB**	n	0.144	-	-	220	66	98	66	-2	74	63	-173	100
4	8	5*	**SB**	n	0.176	-	-	173	70	169	73	4	77	76	-150	78
4	9	7*	**SB**	n	0.104	-	-	365	85	308	94	83	72	87	-250	94
4	8	8*	**SB**	n	0.120	-	-	385	70	309	70	39	79	67	-170	75
4	9	1*	**SB**	y	0.120	-	-	293	74	182	96	43	68	89	-179	100
4	9	4*	**SB**	y	0.120	-	-	194	67	250	92	26	72	90	-291	94
1	3	4	**B**	n	0.317	-72	40	12	69	60	84	-25	12	63	-52	24
1	3	10	**P**	n	0.567	-63	21	53	32	189	44	36	67	44	-95	45
1	3	11	**P**	n	0.317	-29	38	34	41	154	73	13	62	78	-35	80
1	3	12	**P**	n	0.267	-78	45	19	55	424	84	124	73	85	-227	84
1	3	13	**P**	n	0.250	-20	48	41	99	24	100	8	23	99	-13	68
1	3	14	**P**	n	0.300	-23	57	39	99	10	100	11	106	99	-12	62
1	3	15	**P**	n	0.366	-23	37	59	76	47	85	13	87	80	-10	65
2	6	3	**B**	n	0.288	-120	35	80	31	108	32	-12	58	31	-169	32
2	3	1	**B**	n	0.072	-63	71	40	100	52	100	22	50	100	-27	100
2	3	4	**B**	n	0.072	-87	98	55	100	57	100	-23	51	100	-94	43
2	9	5.5*	**B**	n	0.184	-	-	9	3	475	66	140	71	66	-553	64
2	9	7*	**B**	n	0.434	-	-	49	83	288	91	102	69	96	-406	91
2	12	3*	**B**	n	0.167	-	-	23	42	60	100	-29	108	41	-86	100
2	12	4*	**B**	n	0.133	-	-	45	66	-2	100	-26	113	75	-84	100
3	2	1	**B**	n	0.224	-61	56	47	66	14	0	29	28	66	-58	85
3	2	2	**B**	n	0.222	-99	49	61	50	-2	0	14	28	51	-87	100
3	2	3	**B**	n	0.192	-27	25	-5	28	-5	2	-14	40	89	-66	94
3	2	4	**B**	n	0.232	-31	72	5	60	23	100	-12	30	67	-68	87
3	3	4*	**B**	n	0.208	-	-	37	77	297	5	12	14	4	-151	4
3	3	5*	**B**	n	0.088	-	-	23	58	829	100	132	80	100	-341	100
3	3	6*	**B**	n	0.224	-	-	1	64	228	18	31	-5	0	-85	44
4	9	2*	**B**	n	0.184	-	-	126	57	24	4	-18	41	70	-116	3
4	9	5*	**B**	n	0.160	-	-	41	46	63	100	47	96	100	-400	100
4	9	6*	**B**	n	0.128	-	-	-25	73	-27	0	27	29	100	-267	100
4	8	6*	**B**	n	0.104	-	-	84	76	-3	17	-26	46	100	-74	100
4	8	7*	**B**	n	0.144	-	-	149	51	84	100	10	118	50	-119	100

* IP gauge was detached in these events; therefore no IP data are available.

† Angle between maximum principal tension (E1) and E_a gauge component of rosette, where positive angles represent counterclockwise rotation of E1 from the E_a element of the rosette.